Tenth International Conference on Computational Fluid Dynamics (ICCFD10), Barcelona,Spain, July 9-13, 2018 **ICCFD10-191**

Three Dimensional Analysis of Ahmed Body Aerodynamic Performance Enhancement using Steady Suction and Blowing Flow Control Techniques

Bhanu Prakash*, J M Bergada** and F. Mellibovsky*
Corresponding author: bhanu2204@gmail.com

* Department of Physics, UPC-Barcelona, Spain.
** Department of Fluid Mechanics, UPC-Terrassa, Spain.

Abstract: Aerodynamic drag reduction plays a vital role in the reduction of automobiles fuel consumption. Boundary layer physics and its intricate mechanisms that result in flow separation are to be understood and manipulated using active or passive devices, in order to reduce drag. Active flow control has an advantage to be effective in wide range of flow conditions and is analysed in this research. Direct Numerical Simulation (DNS) is performed for computing the flow over ahmed body, which is a simflied car geometry for research activities. Two flow control techniques, steady blowing and steady suction, are implemented for a parametric set inspired from literature. Three simulations are computed i.e., a detailed Baseline flow simulation, then a simulation with steady suction and another with steady blowing. The Reynolds number (Re) based on ahmed body (1/4th scaled) height is 1.48 * 10^4. Steady suction provided a 8.3% drag reduction followed by 3.9% increase with steady blowing, specific to the parametric set considered. The major contribution from this paper is an in-depth analysis of flow physics resulting in this performance and also clearly classifying the differences using suction and blowing actuation.

Keywords: Active Flow Control, Direct Numerical Simulation, Ahmed Body, Boundary layers, Steady suction and Blowing

1 Introduction

The global number of cars and the distance in kilometres flown by air planes is set to nearly double the current quantity by 2040[1]. According to the international energy agency, transport is the second largest sector representing 23% of world CO2 emissions only second to electricity and heat generation (41%) [2]. At highway speeds, Aerodynamic drag is responsible for the largest part of fuel consumption, much higher than tire rolling resistance [3].

Active Flow Control (AFC), based on addition of momentum at precise locations of the boundary layer, is one of the methods with good potential. It is a technique that can add/remove momentum in the boundary layer developed on the surfaces by the incoming flow. Fundamentally, it has the ability to delay/advance the flow separation that can be utilized to obtain aerodynamic performance enhancements. It is conventional to use steady or time varying actuation depending on the performance of interest.

Many relevant numerical studies undertaken using AFC have considered canonical two dimensional configurations, using either DNS and/or LES. Some of the most relevant studies are: Suzuki [4], studied the flow over a hump at Reynolds number (Re) 2300; Dandois et al. [5], evaluated the flow over a rounded backwards facing step at Re 28275; Avdis et al [6], studied a hump configuration at Re near 1e6; Newmann and Wengle [7] considered a backward facing step at Re 3000. Among the experimental studies in canonical configurations, we found relevant to mention Cerretelli and Kirtley [8].

In commercial transport vehicles research, typically 3D-Ahmed Body configuration is considered as a simplified geometry. Although it is very far from realistic vehicles, it will allow us to focus the attention on fundamental physical fluid aspects. Yet, the main flow phenomena it is representative of the one to be found in a real vehicle.

Recent experimental investigations on ahmed body have been focused on studying flows with Re in the order of 10^6. Among them, Aubrun et al [10] considered pulsating actuators at the beginning of the rear inclined surface and Joseph et al [3] considered four flow control configurations, with horizontal actuators near the beginning of the inclined surface and identifying two unsteady phenomena. One, associated with the natural Kelvin-Helmholtz instability of the shear layer and the other with the flapping of the shear layer.

Among the numerical studies of AFC in Ahmed body, Roumeas et al [11] used the Lattice Boltzmann Method to study the flow at Re $2.8*10^6$, the actuation control was performed by a horizontal suction actuator located at the inclined surface upper edge. A significant reduction of the drag was obtained, but the lateral vortices were hardly affected. Krajnovic and Basara [12] studied the effect of a horizontal actuator located at the top of the body at Re $2*10^5$ and using LES, with similar conclusions.

There have been numerous experiments, in wind tunnel, on AFC implementation for 3D Ahmed Body using Pulsed actuators at Reynolds number of O(10^6)[3], Joseph et.al (2012) have observed 8% drag reduction. Similar study by Brunn et. al (2006) at O(10^5) [13] have observed a drag reduction of around 27%. Using steady Blowing at Re of O(10^6) [14] near slant corners have reduced longitudinal or C-pillar vortices but with minimal drag reduction. However, power efficient implementation hasn't been observed in literature. With better understanding of boundary layer physics in terms of impact on specific flow structures and associated instabilities with AFC, significant knowledge can be added to literature. This is one of our main motivation to choose Direct Numerical Simulation approach at a Re of O(10^4)

The novelty in our current research include two aspects. Firstly, influence of AFC on flow structures over inclined surface, lateral edges and near wake is analyzed in detail by resolving all turbulent scales using Direct Numerical Simulation (DNS) methodology. Secondly, the flow control mechanism of steady suction and steady blowing is explained and differentiated.

2 Problem Statement and Methodology

The three dimensional Navier Stokes (NS) Equations for incompressible, viscous and turbulent flow is resolved using DNS. The flow considered is at a height based Reynolds number of $1.48 * 10^4$ with an inlet velocity (U_∞) of 0.207 m/s. The computational domain is developed for a 1/4th scaled Ahmed body with the similar domain dimensions as provided in Tunay et.Al (2016)[15]. The mesh independency is primarily checked by plotting average non dimensional wall units that are below 10, 0.7 and 10 in the stream wise(Δx^+), cross-stream (Δy^+) and in the spanwise direction (Δz^+) of Ahmed body surface respectively. The boundary conditions include velocity inlet, pressure defined outlet, no-slip wall for Ahmed body surface, moving (slip) bottom floor with velocity equivalent to free stream velocity along with symmetry plane for top and side walls of external domain. The bottom floor is considered as slip wall to be closer to the realistic conditions.

A finite volume method (FVM) based open-source solver, icoFoam, within the OpenFOAM solvers framework is used [16]. The temporal and spatial discretization are done using second order numerical schemes. PISO algorithm is used for resolving pressure-velocity coupled equations with Multi-grid solver for pressure and Smooth Solver for velocity.

3 Results and Discussion

The baseline case without any actuation is computed. Although it is conventional to use a stationary floor boundary conditions to match wind tunnel experiments, a moving floor is used in the present research. The boundary layer that develops on the stationary floor impacts the flow over ahmed body with significant impact near the bottom, although the wake flow is found to be insensitive [17]. The moving floor can eliminate this and provide realistic conditions for flow control, in addition to avoiding any numerical dissipation in the simulation that might arise from possible under-resolving of boundary layer over floor.

A total of three cases, simulated using DNS, are considered for analysis. These include Baseline simulation without any flow control (CaseA), steady suction with actuation momentum coefficient (C_μ) = $2.4 * 10^{-3}$ (Case B) and steady blowing with $C_\mu = 2.4 * 10^{-3}$ (Case C). The total grid count of 56 million in Case A and 60 million in Case B and C were considered. The momentum coefficient is defined as $C_\mu = (\rho_j U_j^2 w/\rho U_\infty^2 L)$.

The parameters in the numerator correspond to the jet where ρ_j, U_j and w (0.0025 m)are density, velocity and width of jet respectively. And, in the denominator, ρ, U_∞ (0.207 m/s) are density and velocity of free stream flow respectively and L (0.261 m) is the length of ahmed body. The mesh is also refined in the wake considering the region of the interest to analyse the impact of flow control. The wall units with a strict DNS requirement of $y^+ < 1$ along with the x and z wall units to maintain the desired aspect ratio of cells inside the boundary layer.

With respect to jet parameters, in addition to C_μ, the actuation location is at 0.001 m before the intersection of roof and inclined surfaces. The jet direction is perpendicular to the roof of ahmed body in all cases. The slot from which jet emanates has a width of 0.0025 m (0.96 % L). The velocity of jet is constant and equal to $U_j = U_\infty/2$ in both cases with the sign being positive in the blowing case and negative in the suction case. More importantly, the jet considered is uniform in spanwise direction and a flat profile in the stream wise direction.

The baseline case (case A) is computed for around 20 time units (tU_∞/L), only in the production phase, after eliminating the simulation transients of around 10 time units. The final solution's velocity and pressure fields of case A are used to initialize pressure and velocity for Case B and C. The case C has undergone flow transients before it stabilized and it can be observed from monitoring the drag (C_d) and lift (C_l) coefficient in Figure 1 and 2. Including these transients, a total of 13 and 10 time units are computed for Case B and C respectively.

From figure 1(a), it can be observed that applying steady suction and steady blowing resulted in drag reduction and increase respectively. The mean C_d for Case A (Baseline) is 0.435 where as for Case B(Suction) is 0.399 and Case C (Blowing) is 0.452. For the actuation parameters considered, there is 8.3% decrease and 3.9% increase in mean C_d for suction and blowing respectively. Although mean C_l is not of very much interest for typical commercial cars, the trend is illustrated in figure 1(b) to better study the fundamental analysis of flow control's impact. The mean C_l values are 0.133, 0.203 and -0.183 for cases A, B and C respectively. This means a 52 % increase and 237% decrease in the mean C_l for Suction and Blowing actuation respectively.

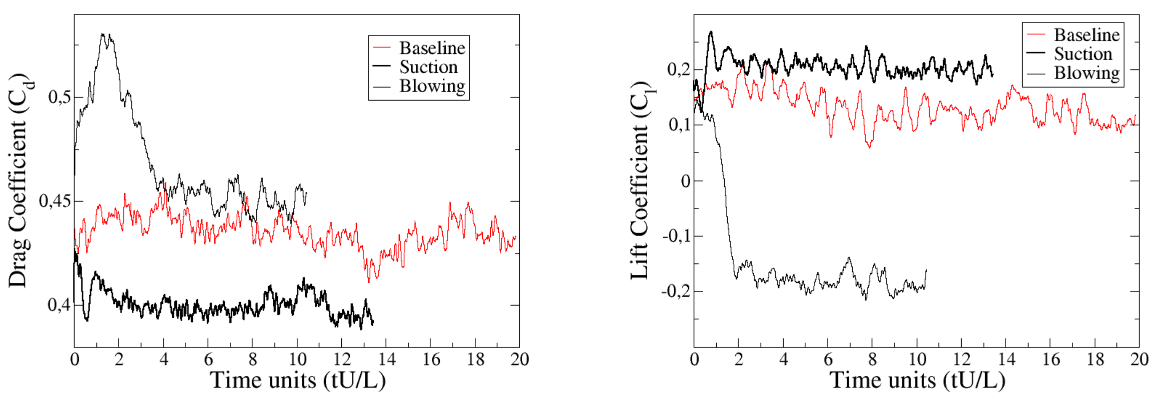

(a) C_d vs time

(b) C_l vs time

Figure 1: Temporal variation of Drag and Lift coefficients for Case A (Baseline), Case B (Suction) and Case C(Blowing

Hence, this necessitates the in-depth analysis of flow physics aspects that are resulting in this aerodynamic performance behaviour. It should also be noted that reducing C_l is of paramount importance in high performing sport cars and hence steady blowing that resulted in significant C_l reduction is also considered for the analysis. Also, the stable trends after simulation transients are a good criterion for relying on the convergence of the simulation

The temporally averaged velocity field visualization in the mid plane section of ahmed body is shown in the Figure 2(a), 2(b) and 2(c) which corresponds to Baseline, Suction and Blowing cases respectively. The mid plane section, with less flow intervention from typical A-pillar and C-pillar vortex structures at lateral edges, provides a broad overview on the impact of flow physics using controlled actuation. It can be noticed clearly that the baseline case is undergoing separation near the immediate downstream of curved front resulting in the turbulent flow over the top surface of ahmed body. A clear flow separation is triggered as it reaches the inclined surface, in the baseline case (figure 2(a)), which has a significant impact on the base pressure there by C_d and C_l. In figure 2(b), the streamwise length of low pressure region in the immediate wake zone is reduced in addition to the size of recirculation vortex inside this region. Also, the flow over inclined surface is well attached as compared to the baseline case. These are the qualitative indications of increased base pressure which is one of the underlying reasons for the drag reduction observed.

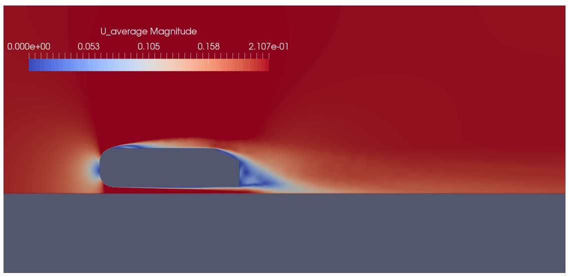

(a) Baseline (Case A)

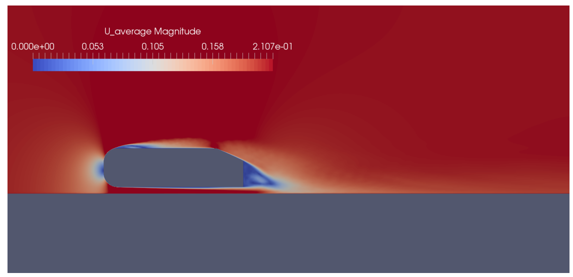

(b) Suction (Case B)

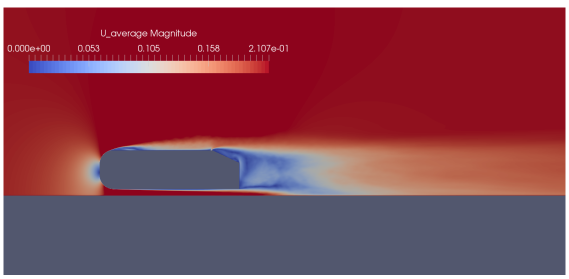

(c) Blowing (Case C)

Figure 2: Time averaged velocity plot at spanwise mid plane section of ahmed body

However, the completely opposite trend in flow physics is observed in the actuation using steady blowing in the figure 2(c), specific to the flow over inclined surface and immediate near wake. In addition, length and turbulent intensity of near and far wake are significantly higher compared to the baseline and suction cases. This translates to lower base pressure resulting in higher C_d. It should also be observed that the flow over top surface is almost the same in all cases because the steady actuation is done very close to the upstream of the inclined surface leaving very low possibility to impact the upstream flow.

The pressure coefficient (C_p) over the ahmed body surface of interest can better provide the quantitative information necessary to validate the trends in C_d and C_l. C_p is computed as (P - P_{atm}) / (0.5* $\rho * U^2$) where P is the pressure averaged temporally and in the span wise direction, P_{atm} is the reference atmospheric pressure, ρ_∞ is the density of fluid and U is the freestream velocity. From the figure 3(a), 3(b) and 3(c), the variation of pressure can be analysed over top, inclined and rear end surfaces of ahmed body, for cases with and without actuation.

As the actuation is performed at the end of the top surface, pressure variation using actuation is observed only close to this region in the figure 3(a). It resulted in higher and lower pressure when using steady blowing and suction respectively. On the inclined surface, a net high pressure is created by steady blowing actuation as compared to the baseline case. So, for steady blowing, the significantly higher net pressure over top and inclined surfaces is resulting in lower C_l with respect to baseline case. For steady suction, although there is a slight net pressure increase over the inclined surface, this was compensated with the net decrease over top surface resulting in C_l increase with steady suction.

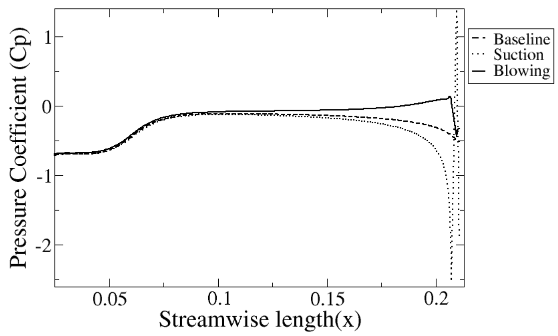

(a) Top surface

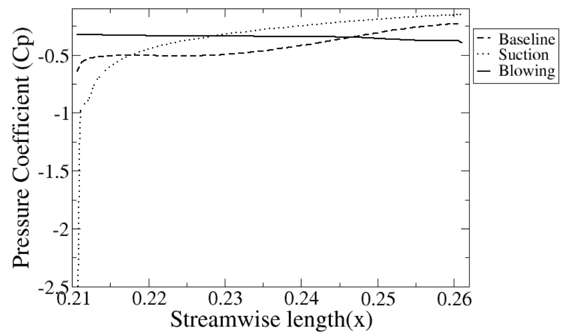

(b) Inclined surface

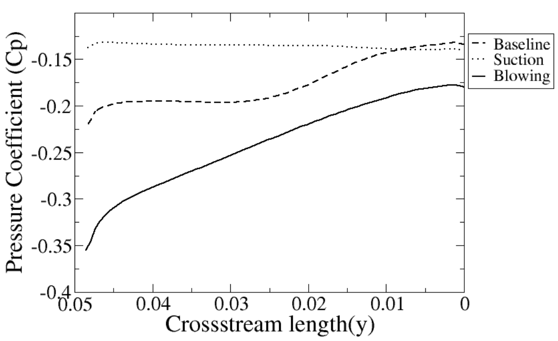

(c) Rear end surface

Figure 3: Time and span wise averaged Pressure Coefficient (C_p) over ahmed body top, inclined and rear end surface

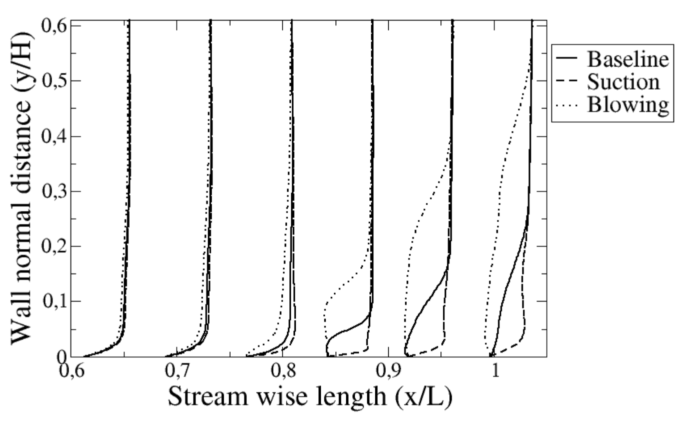

Figure 4: Boundary layer profiles on the top surface (x/L < 0.807) and inclined surface (0.807 < x/L < 1)

On the other hand, from figure 3(c), it is clear that the actuation using suction has shown a base pressure increase over rear end surface. As compared to the baseline case, this increase is resulting in net reduction in C_d. The vice-versa is observed with steady blowing case, where there is a net decrease in the pressure over the rear end surface that increases the net pressure difference between the front and rear ends of ahmed body. This has resulted in a higher C_d value with respect to Baseline case. The trends observed in C_d and C_l are quantitavely deciphered from figures 2 and 3.

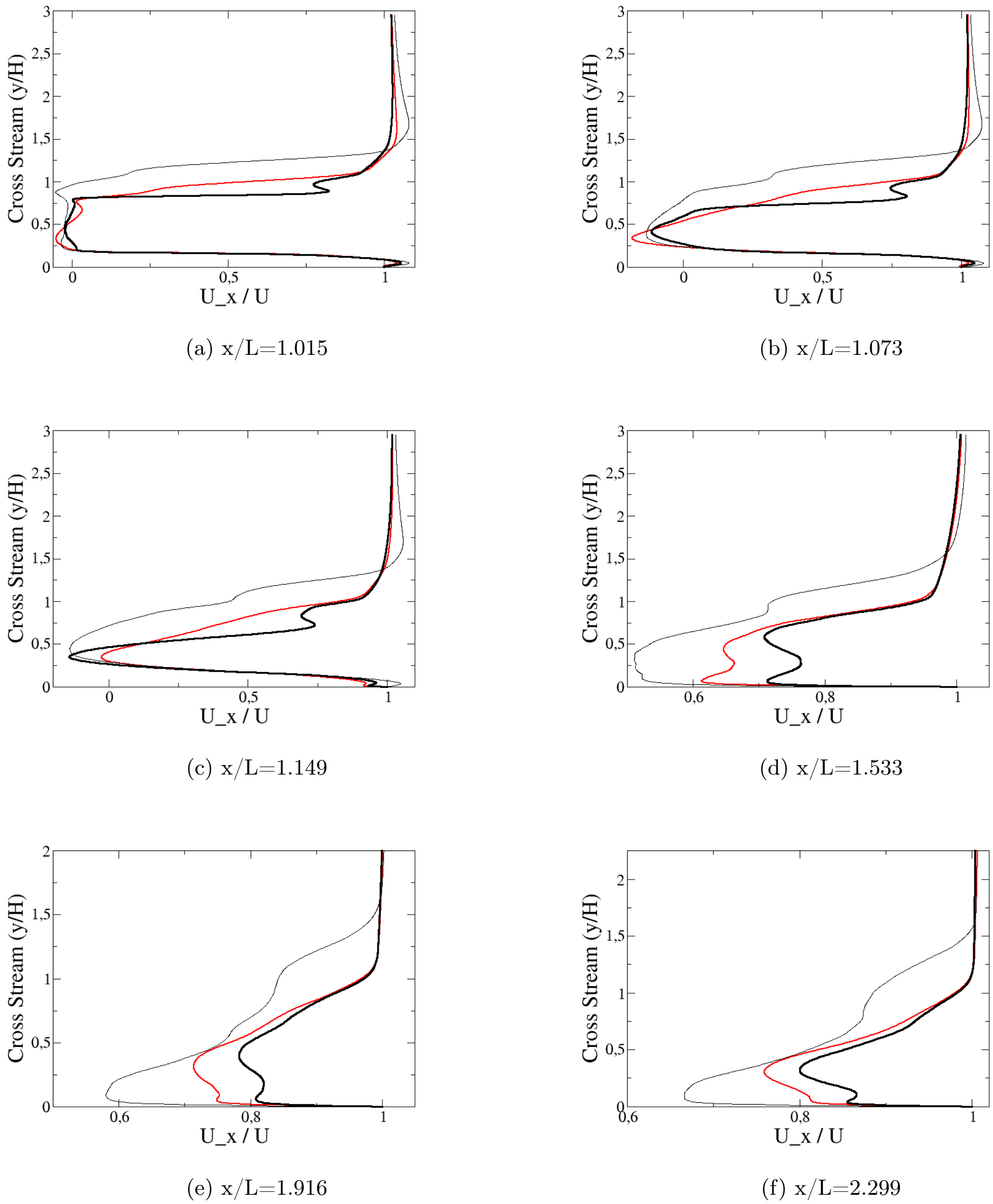

(a) x/L=1.015

(b) x/L=1.073

(c) x/L=1.149

(d) x/L=1.533

(e) x/L=1.916

(f) x/L=2.299

Figure 5: Velocity profiles in the near wake for Baseline (**red line**), Suction(**black thick line**) and Blowing (**black thin line**) cases

To understand the impact on flow physics using actuation, the temporal and span wise averaged boundary layer (BL) velocity profiles are illustrated in figure 4. The streamwise variation in ahmed body geometry include a curved front volume from x/L = 0 to 0.096, top surface from x/L = 0.096 to 0.807 and inclined surface from x/L = 0.807 to 1. BL profiles are plotted near end of top surface and inclined surface. The plots are done on velocity variation normal to wall strictly, including inclined surface region. Until x/L = 0.766, there is very little difference between three cases. To pinpoint a subtle difference until this location, BL thickness using steady blowing is slightly higher. The velocity values are scaled to 5% of original values and hence the shape of the BL profiles has to be noticed.

However, from the end of the top surface, it is very certain about the impact of actuation on the boundary layer. The flow separation from surface is triggered in the baseline case in this region and its impact is being continued on the flow over inclined surface. A clear tendency of the flow to separate followed by turbulent reattachments is evident from x/L = 0.843 to 1 in the figure 4. Hence, it increases the possibility of low base pressure region in baseline case as observed in the figure 3(c).

When using actuation, the BL profiles using suction are very much ideal for low drag conditions with flow almost completely attached over ahmed body top and inclined surfaces. This is a typical situation for low drag and high lift aerodynamic performance as observed in figures 1(a) and 1(b). On the contrary, steady blowing is almost exploding the BL over inclined surface and increasing BL thickness. This results in an increased length of low base pressure region in the immediate wake as observed in figure 2(c).

In figures 5(a) to 5(f), temporal and spanwise averaged wake velocity profiles are computed from x/L = 1.015 to x/L = 2.299 with a focus on the near wake. The velocity deficit in the immediate wake, for baseline case, is evident from figure 5(a) to 5(c) with steady blowing further worsening it and steady suction reducing this deficit. Also the slight increase in the velocity in the crossstream direction with y/H > 1.5 using steady blowing. This shows that the blowing jet after breaking the BL and increasing the thickness, as seen in figure 4, adds momentum further up in the normal direction rather than the immediate wake. Once the flow enters into the near wake region, the velocity profiles are better stabilized as can be seen from figure 5(d) to 5(f). The velocity deficit is significantly reduced with BL suction and hugely increased by blowing into boundary layer. Also, the momentum addition in the normal direction using steady blowing is much clear.

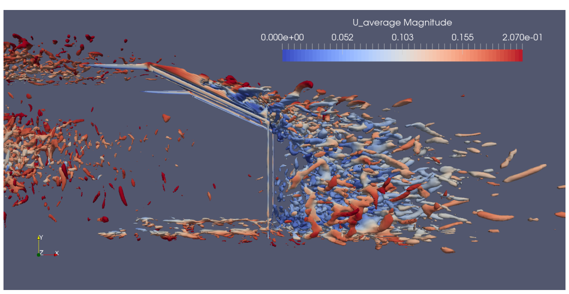

(a) Baseline

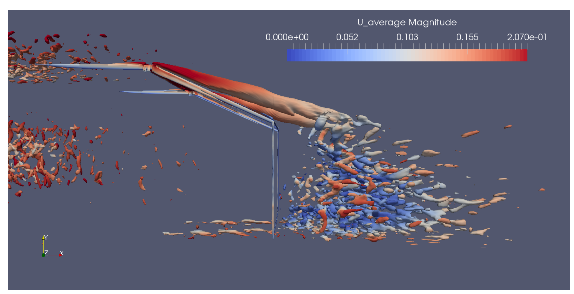

(b) Steady suction

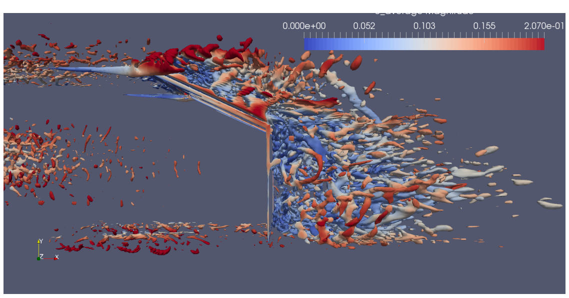

(c) Steady Blowing

Figure 6: Time Averaged Q-criterion iso-contours (Q = 170) for baseline, steady suction and blowing cases

The time averaged Q-criterion iso contours at Q = 170 (coloured by velocity magnitude) for Case A, B and C are presented in figures 6(a) to 6(c). The flow attachment over inclined surface in figure 6(b) causes the drag reduction when actuation is applied using suction. It can be observed that the low pressure region in baseline case (figure 6(a)) over inclined surface and near wake is significantly reduced. Where as in figure 6(c), the incoming free stream flow interaction with blowing jet has pushed the flow away from inclined surface and thereby creating a low pressure region that resulted in significant pressure drag contributions to C_d. This has led to net drag increase with blowing compared to baseline case. In addition, the c-pillar vortices are being strengthened with suction while they are being broken and introduced into the flow over inclined surface in the case of Blowing. As the actuation is being done close to the end of top surface, a very little impact is being noticed on A-pillar vortices. The immediate near wake phenomena observed and explained in the previous sections can be further validated here.

4 Conclusion and Future Work

Direct Numerical simulation is performed for active flow control implementation over ahmed body. With steady suction and steady blowing, 8.3% decrease and 3.9% increase in C_d are observed respectively. Although C_l is not of specific interest, a 52% increase and 237% decrease is noticed with suction and blowing actuations respectively. It should be noted about the low Reynolds number regime when considering this aerodynamic performance.

This performance is obtained due to the flow physics manipulation when using actuation. The reduction in C_d is obtained because of multiple aspects. The mid-plane velocity profile in figure 2 illustrates that length of recirculation region in the near wake is reduced in addition to the size of circulating bubble inside this region, which indicates an increase in base pressure. Near Wake velocity deficit is also reduced as seen clearly in figure 5(d) to 5(f). These effects are caused by flow reattachment over the inclined surface after boundary layer (BL) suction near the end of ahmed body top surface as observed in the BL velocity profiles in figure 4. Also, strength of C-pillar vortices near the lateral edges of inclined surface is increased. Though the reason for this needs to be studied further, the uniform spanwise actuation over top surface might be the cause of this effect.

Regarding the steady blowing, although injecting momentum into the boundary layer, didn't result in the flow reattachment over inclined surface or near wake flow improvements. The boundary layer is being disrupted clearly as seen in the BL velocity profiles from figure 4. And momentum additions are away from the ahmedbody in the cross flow direction. So, this resulted in the increased low pressure region in the near wake resulting in higher drag compared to baseline simulation. However, there is a pressure increase on the top and inclined surface. Decrease in the lift, though not useful for conventional commercial vehicles, is one aspect which could be a possible solution for downforce increments in high performing cars. But, tests needs to be done at high Reynolds numbers.

As future work, the full scale turbulence resolved by Direct numerical simulation will be taken advantage of in this work and turbulent statistics are to be analysed in detail. Also, couple of additional cases of steady blowing and suction that were computed and not presented here will be considered for post-processing. Using these insights, periodic blowing and suction using DNS at the same Reynolds number can be implemented in the near future.

5 Acknowledgements

We are very thankful to the Red Espanola de Supercomputacion (RES) network of supercomputers for providing the necessary computing resources for this project. Also, this work is conducted as part of the Spanish government funded research grant, FIS2016-77849-R, in the duration of 2017-2020.

References

[1] World economic forum. `https://www.weforum.org/agenda/2016/04/the-number-of-cars-worldwide-is-set-to-double-by-2040`. Accessed: 2018-06-14.

[2] International energy agency report. `http://www.iea.org/media/statistics/co2highlights.pdf`. Accessed: 2018-06-14.

[3] Pierric Joseph, Xavier Amandolèse, and Jean-Luc Aider. Drag reduction on the 25 slant angle ahmed reference body using pulsed jets. *Experiments in fluids*, 52(5):1169–1185, 2012.

[4] Takao Suzuki. Effects of a synthetic jet acting on a separated flow over a hump. *Journal of Fluid Mechanics*, 547:331–359, 2006.

[5] Julien Dandois, Eric Garnier, and Pierre Sagaut. Numerical simulation of active separation control by a synthetic jet. *Journal of Fluid Mechanics*, 574:25–58, 2007.

[6] Alexandros Avdis, Sylvain Lardeau, and Michael Leschziner. Large eddy simulation of separated flow over a two-dimensional hump with and without control by means of a synthetic slot-jet. *Flow, turbulence and combustion*, 83(3):343–370, 2009.

[7] Jens Neumann and Hans Wengle. Les of controlled turbulent flow over a rounded step. In *Direct and Large-Eddy Simulation V*, pages 557–564. Springer, 2004.

[8] Ciro Cerretelli and Kevin Kirtley. Boundary layer separation control with fluidic oscillators. *Journal of Turbomachinery*, 131(4):041001, 2009.

[9] Timothée Chabert, Julien Dandois, and Éric Garnier. Experimental closed-loop control of flow separation over a plain flap using slope seeking. *Experiments in fluids*, 55(8):1797, 2014.

[10] Sandrine Aubrun, Jonathan McNally, Farrukh Alvi, and Azeddine Kourta. Separation flow control on a generic ground vehicle using steady microjet arrays. *Experiments in fluids*, 51(5):1177–1187, 2011.

[11] Mathieu Rouméas, Patrick Gilliéron, and Azeddine Kourta. Drag reduction by flow separation control on a car after body. *International journal for numerical methods in fluids*, 60(11):1222–1240, 2009.

[12] Siniša Krajnović and Branislav Basara. Les of the flow around ahmed body with active flow control. In *Turbulence and Interactions*, pages 247–254. Springer, 2010.

[13] A Brunn and W Nitsche. Drag reduction of an ahmed car model by means of active separation control at the rear vehicle slant. *New Results in Numerical and Experimental Fluid Mechanics V*, pages 249–256, 2006.

[14] A Brunn, E Wassen, D Sperber, W Nitsche, and F Thiele. Active drag control for a generic car model. In *Active Flow Control*, pages 247–259. Springer, 2007.

[15] Tural Tunay, Bulent Yaniktepe, and Besir Sahin. Computational and experimental investigations of the vortical flow structures in the near wake region downstream of the ahmed vehicle model. *Journal of Wind Engineering and Industrial Aerodynamics*, 159:48–64, 2016.

[16] Henry G Weller, Gavin Tabor, Hrvoje Jasak, and Christer Fureby. A tensorial approach to computational continuum mechanics using object-oriented techniques. *Computers in physics*, 12(6):620–631, 1998.

[17] Siniša Krajnović and Lars Davidson. Influence of floor motions in wind tunnels on the aerodynamics of road vehicles. *Journal of wind engineering and industrial aerodynamics*, 93(9):677–696, 2005.